DOI: 10.14529/jsfi260104

Comparative Molecular Dynamics Study of E- and Z-Biliverdin-IXα Binding to Human Serum Albumin

Igor V. Polyakov[1], *Maria G. Khrenova*[1]

Human serum albumin (HSA) is the main transporter of a wide range of endogenous ligands, including linear tetrapyrrolic bile pigments. Despite many experimental and theoretical studies, the detailed binding modes of linear tetrapyrroles in HSA remain not fully understood. Here, we investigate the interaction of 4Z,15E and 4Z,15Z biliverdin-IXα with HSA by classical molecular dynamics and machine learning. Starting from the crystallographic complex of HSA with 4Z,15E bilirubin-IXα, we construct models for both biliverdin isomers and explore their conformational space in the initial binding site. We analyse protein-ligand contacts, conformational flexibility, and the populations of distinct binding poses using clustering of interaction fingerprints. The results reveal both shared and isomer-specific interaction patterns between biliverdin and HSA. Several conserved contacts are maintained in both complexes, while distinct differences in contact occupancies and binding pocket conformations are observed between the E- and Z-isomers. Overall, this study provides a consistent molecular level picture of how biliverdin isomers interact with HSA and demonstrates a practical workflow for analysing flexible protein-ligand complexes by combining molecular dynamics with interaction fingerprint clustering.

Keywords: albumin, biliverdin, bilirubin, molecular dynamics, clustering.

Introduction

Human serum albumin (HSA) is the main transport protein in blood plasma which carries out an important task of binding and carrying a wide range of compounds, including fatty acids, bile pigments, hormones, and many drugs [2]. Because of its flexible structure, albumin can form stable complexes with ligands of different chemical nature, significantly influencing their bioavailability, distribution, and metabolism in the organism [5, 9]. HSA is a monomeric protein composed of three domains (I–III), and each domain is divided into two subdomains (A and B). Several functionally important binding sites are located inside these domains (Fig. 1), and the most studied ones are Sudlow site I and Sudlow site II in subdomains IIA and IIIA, which are mainly associated with aromatic and hydrophobic ligands [10]. Albumin also contains additional hydrophobic pockets and cavities (Fig. 1) that can bind large and flexible molecules, and the protein conformation can adapt to the chemical nature of the ligand. Bilirubin and biliverdin are endogenous bilins, tetrapyrrolic chromophores formed during heme catabolism. Biliverdin is produced in the oxidative cleavage of heme by heme oxygenase and is then reduced to bilirubin by biliverdin reductase. In blood plasma, bilirubin is almost completely bound to albumin [21], which prevents its precipitation and toxic effects on tissues. The bilirubin molecule is highly conformationally flexible, forms intramolecular hydrogen bonds [15], and can exist in different isomeric forms, mainly as 15Z and 15E isomers (Fig. 1). Isomeric states of bilin chromophores can significantly influence their physicochemical properties and the mode of interaction with proteins, which is important both in biophysical and clinical contexts, for example for phototherapy of hyperbilirubinemia [14].

Experimental studies of bilirubin binding to human serum albumin usually employ spectroscopic methods (such as fluorescence spectroscopy, circular dichroism, and absorption) and kinetic measurements, which provide estimates of binding constants and confirm the presence

[1]Department of Chemistry, Lomonosov Moscow State University, Moscow, Russian Federation

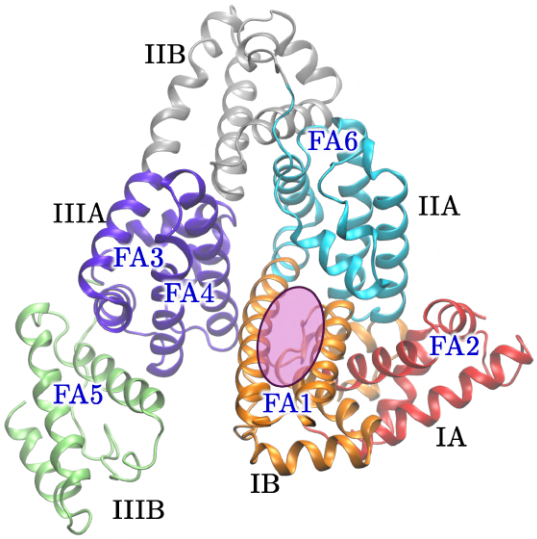

(a) Different ligand binding sites in albumin, the heme binding site is highlighted

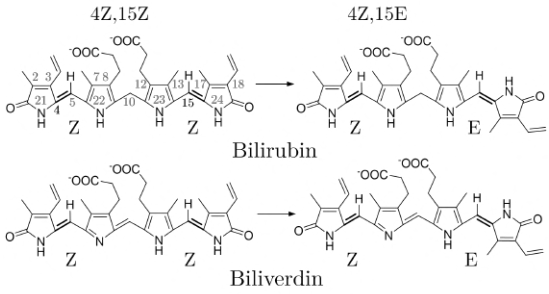

(b) Structures of the main isomers of bilirubin and biliverdin

Figure 1. Protein and ligands

of a high affinity bilirubin-albumin interaction [3, 14]. These approaches give important quantitative parameters, but they have limited ability to resolve the three dimensional architecture of the complex, to describe in detail the dynamic structural changes of the ligand and the protein during binding, and to clarify the specific role of individual amino acid residues in complex stabilization. In this work, we inspected the current state of structural data in the Protein Data Bank (PDB), which contains many experimentally determined three dimensional structures of human serum albumin complexes with different endogenous and exogenous ligands, including fatty acids, steroid hormones, and various pharmacologically active molecules. At the same time, structural data on albumin complexes with bilin chromophores are very limited. At present, the only experimentally resolved atomic structure of a human serum albumin complex with bilirubin is the structure with PDB ID 2VUE, where albumin is crystallised with 4Z,15E bilirubin IXα [28] (the identified binding site is highlighted in Fig. 1).

It was shown that in the albumin complex bilirubin is located in a deep, mainly hydrophobic cavity formed by amino acid residues of subdomain IB. Structural analysis indicates that the bilirubin binding disturbs the Sudlow site I region, but the geometry of the cavity and the interaction pattern differ significantly from typical albumin-drug complexes. In particular, bilirubin adopts an extended and curved conformation inside the cavity, which requires local rearrangement of amino acid side chains and demonstrates pronounced conformational plasticity of the protein. Compared to complexes with fatty acids or small aromatic ligands, bilirubin interacts with albumin not only through nonpolar contacts but also via hydrogen bonds with nearby polar and charged residues, which stabilise its conformation in the bound state. The authors of the crystallographic study clearly show [28] that under crystallisation conditions bilirubin binds in one dominant site. However, they also note that several earlier studies suggest a more complex binding behaviour that may include additional, lower affinity or transient binding modes. The absence of direct structural observation of these states can be related to their low population and high conformational mobility of the ligand; therefore, alternative bilirubin-albumin binding

modes that may exist in solution remain outside the scope of experimental structural data but can be explored by atomistic molecular modelling.

Spectroscopic studies have demonstrated that, like bilirubin, biliverdin can also bind to HSA, thus affecting the intrinsic tryptophan fluorescence and influencing the binding of other ligands by competition for the site [16, 26]. However, no experimentally resolved crystal structures of HSA-biliverdin complexes are currently available in the literature, so the exact localisation and binding pattern of biliverdin remain unknown.

Molecular modelling and molecular dynamics (MD) [27] simulations are now widely and routinely used to study protein-ligand and protein-protein complexes. Nevertheless, existing computational studies of albumin complexes with bilin chromophores are very limited [7, 19, 23]. These works usually rely on relatively short molecular dynamics trajectories and do not include a systematic analysis of the ligand conformational ensemble and its interactions with the protein. Modern microsecond scale atomistic models of HSA-bilirubin/biliverdin complexes, with statistically reliable averaging over multiple trajectories, are not yet available. For this reason, the application of current molecular modelling techniques to investigate the structure and dynamics of the HSA-biliverdin complex is a relevant task. Such an approach can reveal specific features of ligand conformational behaviour, differences between its isomeric forms, and the key amino acid residues and interactions that determine the stability of the protein-ligand complex. An additional important aspect is the development of a workflow that allows for automated analysis of such protein-ligand systems. The article is organized as follows. First, we describe the molecular model setup for the HSA-biliverdin system followed by a description of the molecular dynamics protocol. The analysis and discussion of the obtained results is carried out with both statistical approaches and machine learning algorithms.

1. Protein-Ligand Complex Model Setup

As the starting structure for our model, we used the heavy atom coordinates from the Protein Data Bank entry 2VUE [28], since bilirubin is the ligand most similar in structure to biliverdin and no HSA-biliverdin structures are available in the PDB. Using HSA structures with small ligands as starting points was considered problematic, because docking of extended and flexible tetrapyrrolic ligands is a nontrivial task, especially when taking into account the intrinsic mobility of the albumin structure. In the original crystal structure, a region with missing electron density corresponding to residues 79–88 is present. Although this fragment is not part of the bilirubin binding site and does not directly affect complex formation, it was rebuilt using the tools of the Rosetta molecular modelling package [1]. Since PDB ID 2VUE contains only a small number of crystallographic water molecules, we performed additional solvation with the Dowser++ program [20], which is designed to predict energetically favourable positions of water molecules in protein cavities. A total of 365 water molecules were placed in the structure according to predicted positions.

We used the CHARMM36m [12] force field to describe HSA, since it is widely applied for protein simulations and provides good accuracy for structural and dynamical properties. Parameters for bilirubin were generated with the CHARMM general force field CGenFF [25], which is designed for small organic molecules within the CHARMM framework. Because of the high conformational flexibility of biliverdin and the lack of previously published parameters, we performed an additional validation of the CGenFF parameters. For this purpose, we prepared a separate test system containing a single biliverdin molecule embedded in a box of 200 TIP3 water

molecules. The biliverdin structure was first optimised at the molecular mechanics level and then refined by a hybrid QM/MM approach using the NAMD/TeraChem software and modified interface [18, 24]. The QM part comprised the biliverdin molecule, while water molecules were treated by molecular mechanics. QM part was computed with the wB97X D3/6 31G** [17] level of theory. The good agreement between the optimised geometries indicates that the selected parameters provide an adequate description of biliverdin.

The complete simulation system was assembled with the PSFGEN module of VMD [13]. Protonation of amino acid side chains was carried out according to a neutral pH: histidine residues were treated as neutral, aspartate and glutamate residues as deprotonated, lysine and arginine residues were protonated. Disulfide bridges were manually introduced between the following cysteine residue pairs: 53–62, 75–91, 90–101, 124–169, 168–177, 200–246, 245–253, 265–279, 278–289, 316–361, 360–369, 392–438, 437–448, 461–477, 476–487, 514–559, and 558–567. The protonated HSA-biliverdin complex, including the predicted structural water molecules, was then placed in a cubic simulation water box such that the minimum distance from any protein atom to the box boundary was at least 10 Å. To mimic physiological conditions, sodium and chloride ions were added to reach a NaCl concentration of 0.15 mol/L, and their total number was adjusted to ensure overall charge neutrality of the system.

2. Molecular Dynamics Protocol

Molecular dynamics simulations were performed with the NAMD software version 3.0.2 [22]. Model systems were simulated in the isothermal-isobaric ensemble (NPT, P = 1 atm, T = 300 K) using Langevin dynamics. The SHAKE and SETTLE algorithms were utilized to constraint bonds involving hydrogen atoms, which allowed for the use of 2 fs integration time step. Periodic boundary conditions were enforced: long range electrostatic interactions were treated by the particle mesh Ewald algorithm, and a cutoff of 12 Åwas applied for exact electrostatics.

The equilibration protocol consisted of several consecutive stages. In the first stage, only the solvent was relaxed, while the coordinates of the protein and ligand were kept fully fixed for 5 ns, in order to remove unfavourable contacts of water with the protein and ligand surface. Next, the fixed positional constraints were replaced by harmonic restraints with a force constant of 1 kcal/(mol·Å^2) applied to all heavy atoms of the protein and biliverdin for the next 10 ns of simulation to allow for a "soft" start. In the production stage, all constraints were removed except for harmonic restraints with the same force constant applied to the Cα atoms of five N terminal and five C terminal residues of the protein chain, which were used to prevent global drift of the protein and excessive motion of termini.

To study the dynamics of the HSA-biliverdin complex, several independent molecular dynamics trajectories for different isomeric forms of the ligand were computed. For the 15E isomer, which corresponds to the configuration present in the PDB ID 2VUE crystal structure [28], four independent trajectories were calculated, and four trajectories were also obtained for the native 15Z isomer. Each trajectory was 18 hundred nanoseconds long, thus the total simulation time exceeded 14 μs. The use of multiple independent trajectories provided statistically meaningful averaging and a more complete description of the conformational ensemble of the protein-ligand complex.

3. Results and Discussion

To enable the analysis of molecular dynamics trajectories, we first aligned all frames to the protein backbone, which removes the effect of global protein motions and allows focusing on local dynamics of the complex. However, the total amount of data included hundreds of thousands of frames, so manual inspection of such volume is not possible even for a human expert. Therefore, we applied computational methods to extract useful information from the molecular statistics, including analysis of ligand conformations, mobility of protein residues, and protein-ligand contacts. The root-mean-square deviation (RMSD) values for the protein backbone in the E and Z models were 3.25 ± 0.67 Å and 3.68 ± 0.77 Å, respectively, while for heavy atoms of biliverdin they were 3.49 ± 1.05 Å and 3.44 ± 0.68 Å. The calculated RMSF values per protein residue are shown in Fig. 2, and per atom groups of biliverdin – in Fig. 3. The

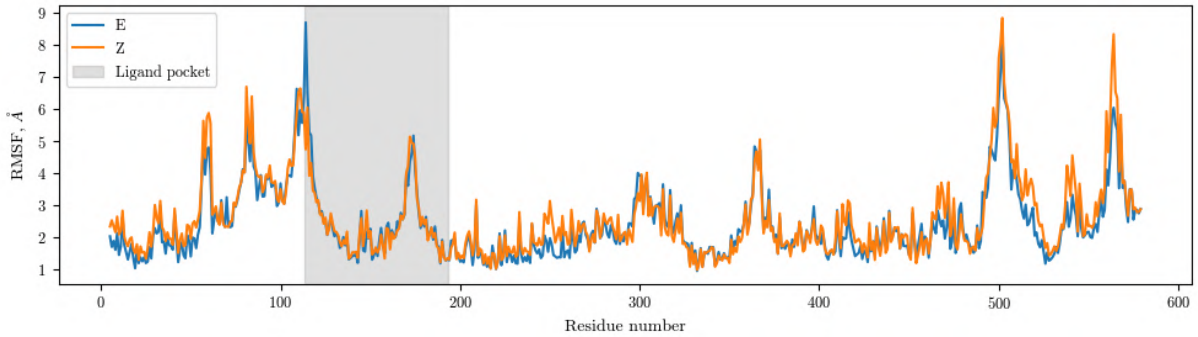

Figure 2. Protein residues RMSF values for the E- and Z-models. The original ligand pocket is highlighted

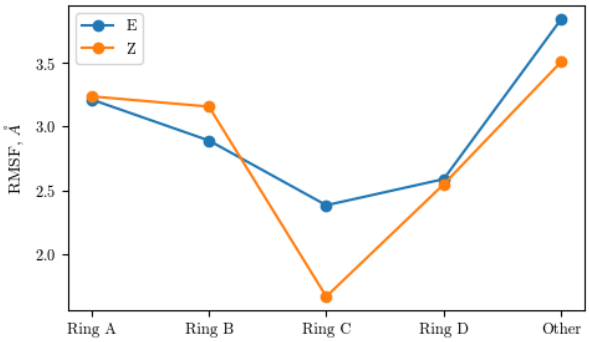

Figure 3. RMSF values for different atom groups of biliverdin

most noticeable difference between the models is observed in the RMSF of residue Arg114 in the chromophore pocket, located on the loop connecting parts of domain I (IA and IB), as well as ring C of biliverdin – however, this information is clearly not enough for comparative evaluation of the models. The most direct and simple method to assess conformational diversity of the studied complexes is QT-clustering [6] (Quality Threshold Clustering) implemented in VMD [13], which can be performed based on RMSD of heavy atoms of the ligand and surrounding amino acid residues. Unfortunately, since biliverdin is a rather flexible ligand and its conformation and position in the protein pocket change significantly along the trajectories, this simple method did not yield satisfactory results – a more precise tool is required to identify patterns of protein-ligand contacts.

Therefore, to detect key interactions of biliverdin with HSA amino acid residues, we used the MDAnalysis [11] package together with the ProLIF module [4]. The algorithm allows for efficient extraction and analysis of various contact descriptors for long MD trajectories. Specifically: Anionic – an interaction where the ligand acts as an anion (negatively charged) and the protein residue as a cation (for example, interaction of the ligand carboxyl group with lysine or arginine); HBDonor – the ligand donates a proton in a hydrogen bond, while the protein accepts it; HBAcceptor – the ligand has an electronegative atom with a lone pair that attracts hydrogen from the protein; Hydrophobic – hydrophobic contacts between nonpolar atoms (carbon, sulfur, halogens), recorded by default at interatomic distances up to 4.5Å; PiCation – interaction between a positively charged group and an aromatic ring; VdWContact – the least specific descriptor that records simple approach of any atoms to the sum of their van der Waals radii with a small tolerance. The detected contacts are shown schematically in Fig. 4, where the colour coding corresponds to the different interaction types described above (VdWContact – golden, PiCation – purple, HBDonor/Acceptor – blue, Anionic – dark blue), the line thickness reflects contact frequency, and contacts observed in less than 20% of trajectory frames were excluded from the scheme. The schemes in Fig. 4 show that several charged residues (Glu141,

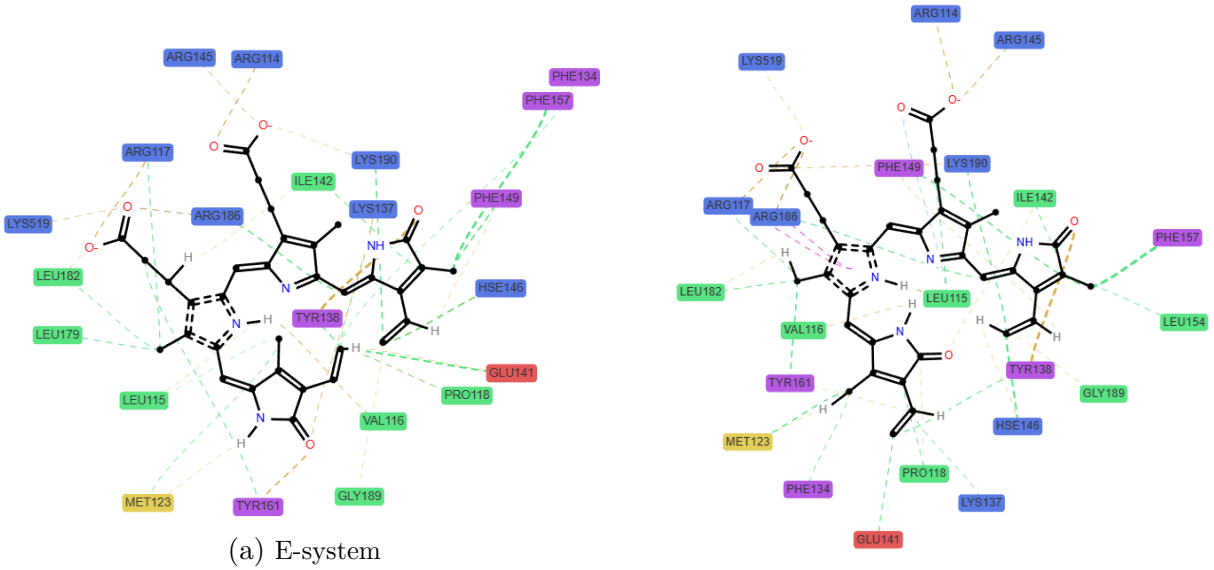

(a) E-system

(b) Z-system

Figure 4. Schematic representation of protein-ligand contacts detected in the molecular dynamics trajectories

Arg114/117/145/186, Lys190) and aliphatic residues (Val116, Leu115/182, Pro118, Ile142), as well as aromatic residues of the protein (Tyr138/161, Phe134/149/157), make contacts with both 15Z and 15E biliverdin. These data are quantified in Tab. 1 and Tab. 2, which list the most similar and most different contacts between the systems, considering the average occupancy based on the score. The score is calculated in percent as the average occupancy multiplied either by the distance from the modulus of occupancy difference to unity (Tab. 1) or by the modulus of occupancy difference (Tab. 2). Although this type of analysis reveals both average similar and average different interactions with residues of the protein chromophore pocket, it still does not provide a clear description of conformational diversity in the systems and does not allow for selection of representative structures for further comparative analysis. Therefore, we performed clustering based on the extracted contact data.

Table 1. Top score similar contacts along the trajectories for albumin model systems with 15E- and 15Z-biliverdin isomers

residue	His146	Ile142	Phe149	Lys190	Tyr138	Arg186	Pro118	Arg117	Phe157	Leu115
E_occ	95	99	91	84	84	77	72	74	66	58
Z_occ	97	94	97	91	81	93	83	95	83	58
score	93	92	88	81	80	72	69	67	61	58

Table 2. Top score different contacts along the trajectories for albumin model systems with 15E- and 15Z-biliverdin isomers

residue	Glu141	Tyr161	Met123	Arg117	Arg186	Tyr161	Phe157	Tyr138
E_occ	91	43	54	71	55	66	66	92
Z_occ	36	78	84	95	77	38	83	79
score	35	21	21	20	15	14	13	11

For each system, we selected a subset of frames by uniform subsampling to limit the total number of analysed frames to 3000. For each selected frame, a binary interaction fingerprint describing ligand-protein contacts was computed using the ProLIF framework, which produces a bit vector encoding the presence or absence of specific interaction types between the ligand and protein residues. Pairwise similarity between fingerprints was quantified with the Tanimoto coefficient, and a distance matrix was constructed as $d_{ij} = 1 - S_{ij}$. Hierarchical agglomerative clustering was carried out using the complete linkage method. The optimal number of clusters was found by maximising the silhouette score over cluster numbers from 2 to 11. For each cluster, the population was calculated as the fraction of frames assigned to that cluster. A representative frame was taken as the structure with maximum total similarity to all other frames in the same cluster; these structures were utilized for visualisation. The process resulted in 4 clusters for the E-system and 5 for the Z-system, with populations of 0.25, 0.37, 0.15, 0.23 and 0.47, 0.12, 0.04, 0.22, 0.15 for the E- and Z-system, respectively. These populations indicate significant conformational diversity for the Z-isomer, where the dominant cluster accounts for less than half of all frames, while for the E-isomer the main cluster is close to one third of frames. Alignment of representative frames from molecular dynamic simulations for both systems is shown in Fig. 5 and Fig. 6, black arrows indicate residues that considerably change spatial location. The performed analysis reveals significant conformational diversity both between the E- and Z-systems and within each of these systems. For example, in the most populated clusters of the E-system (cluster 2 [0.37] and cluster 1 [0.25]), the main differences (modulus of contact occupancy difference over 0.5) are observed for contacts with Arg114 (0.7), Met123 (0.6), Phe134 (0.7), Lys137 (0.6), Tyr138 (1.0), Phe157 (0.9), Tyr161 (0.7), Leu179 (0.6), and Leu182 (0.9). Similar values for the Z-system clusters (1 [0.47] and 4 [0.22]) include: Asn111 (0.7), Pro113 (0.6), Arg114 (1.0), Leu115 (1.0), Val116 (0.5), Arg117 (0.9), Lys137 (0.5), Tyr138 (0.7), Arg145 (1.0), His146 (0.6), Leu182 (0.6), Arg186 (0.8), Lys190 (1.0), Lys519 (0.7), Glu520 (0.8), Ile523 (0.6). When comparing the most populated clusters between E (2 [0.37]) and Z (1 [0.47]) systems, the largest absolute differences in contact frequencies were found for Glu141 (0.7), Leu115 (0.6), Leu179 (0.6), Met123 (0.6), and Tyr161 (0.6). Since we believe in the importance of transparency and reproducibility for any computational publication, including this work, the complete workflow used here, as well as the trajectory data and representative frames, are available in the public Zenodo repository [8].

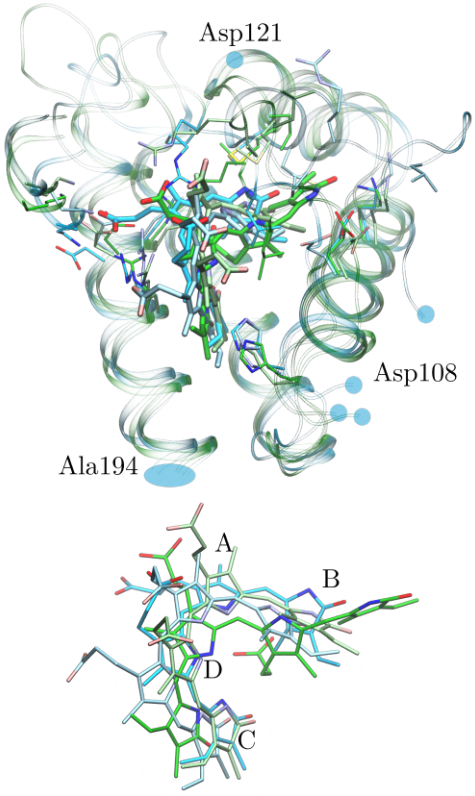

(a) Alignment of entire structures by protein backbone

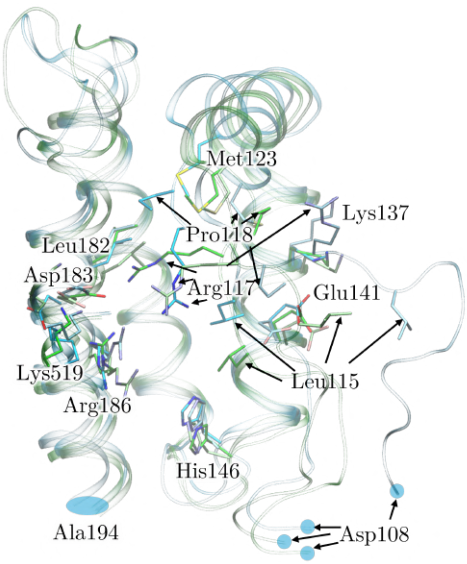

(b) Amino acid residues that interact with biliverdin

Figure 5. E-system representative frames from clustering

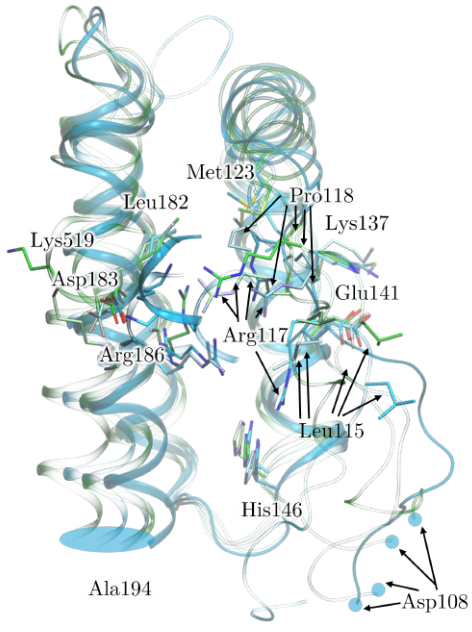

(a) Amino acid residues that interact with biliverdin

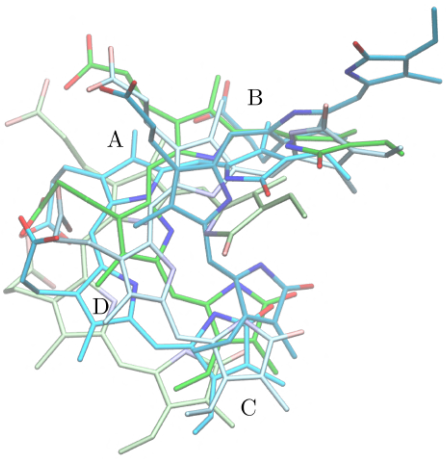

(b) Biliverdin molecules in the aligned structures

Figure 6. Z-system representative frames from clustering

Conclusion

In this work we calculated a set of long molecular dynamics trajectories of the human serum albumin complex with the biliverdin ligand. A thorough analysis of the trajectories was conducted for both 15E- and 15Z-biliverdin isomers showing that biliverdin remains located in the original albumin bilirubin cavity as defined in the PDB ID 2VUE experimental structure throughout the simulation. The biliverdin ligand demonstrates significant positional fluctuations within the cavity and adopts different conformations for both isomeric forms of biliverdin, 15E and 15Z. Examination of the protein-ligand contact network along the trajectories revealed top similar and top different contacts for both model systems. Hierarchical agglomerative clustering based on the pairwise similarity between fingerprints allowed us to quantify not only differences between the binding modes of the isomers but also substantial variation of contacts within individual trajectories and extract representative frames for structural comparison. Therefore, the molecular modeling methods and trajectory analysis techniques applied here can be used in future studies to model properties such as absorption spectra of protein-ligand systems, since accurate prediction of these properties requires consideration of the full conformational ensemble rather than a single structure. The computational workflow we developed, based on the MDAnalysis and ProLIF libraries, simplifies the analysis of protein-ligand system molecular dynamics trajectories. The workflow is available free of charge in the public Zenodo repository [8].

Acknowledgements

The work was conducted under the state assignment of Lomonosov Moscow State University 121031300176-3. The research was carried out using the equipment of the shared research facilities of HPC computing resources at Lomonosov Moscow State University including Istok computing system (Agreement 075-15-2025-541).

References

1. Alford, R.F., Leaver-Fay, A., Jeliazkov, J.R., *et al.*: The Rosetta all-atom energy function for macromolecular modeling and design. Journal of Chemical Theory and Computation 13(6), 3031–3048 (2017). https://doi.org/10.1021/acs.jctc.7b00125

2. Ashraf, S., Qaiser, H., Tariq, S., *et al.*: Unraveling the versatility of human serum albumin – a comprehensive review of its biological significance and therapeutic potential. Current Research in Structural Biology 6, 100114 (2023). https://doi.org/10.1016/j.crstbi.2023.100114

3. Berde, C., Hudson, B., Simoni, R., Sklar, L.: Human serum albumin. Spectroscopic studies of binding and proximity relationships for fatty acids and bilirubin. Journal of Biological Chemistry 254(2), 391–400 (1979). https://doi.org/10.1016/S0021-9258(17)37930-9

4. Bouysset, C., Fiorucci, S.: ProLIF: a library to encode molecular interactions as fingerprints. Journal of Cheminformatics 13(1) (Sep 2021). https://doi.org/10.1186/

s13321-021-00548-6

5. Catalano, C., Lucier, K.W., To, D., *et al.*: The CryoEM structure of human serum albumin in complex with ligands. Journal of Structural Biology 216(3), 108105 (2024). https://doi.org/10.1016/j.jsb.2024.108105

6. Daura, X., Conchillo-Solé, O.: On quality thresholds for the clustering of molecular structures. Journal of Chemical Information and Modeling 62(22), 5738–5745 (2022). https://doi.org/10.1021/acs.jcim.2c01079

7. Díaz, N., Suárez, D., Sordo, T.L., Merz, K.M.: Molecular Dynamics Study of the IIA Binding Site in Human Serum Albumin: Influence of the Protonation State of Lys195 and Lys199. Journal of Medicinal Chemistry 44(2), 250–260 (2001). https://doi.org/10.1021/jm000340v

8. European Organization for Nuclear Research, OpenAIRE: Zenodo (2013). https://doi.org/10.5281/zenodo.18630027

9. Fasano, M., Curry, S., Terreno, E., *et al.*: The extraordinary ligand binding properties of human serum albumin. IUBMB Life 57(12), 787–796 (2005). https://doi.org/10.1080/15216540500404093

10. Ghuman, J., Zunszain, P.A., Petitpas, I., *et al.*: Structural basis of the drug-binding specificity of human serum albumin. Journal of Molecular Biology 353(1), 38–52 (2005). https://doi.org/10.1016/j.jmb.2005.07.075

11. Gowers, R., Linke, M., Barnoud, J., *et al.*: MDAnalysis: A Python Package for the Rapid Analysis of Molecular Dynamics Simulations. In: Proceedings of the 15th Python in Science Conference. p. 98–105. SciPy (2016). https://doi.org/10.25080/majora-629e541a-00e

12. Huang, J., Rauscher, S., Nawrocki, G., *et al.*: CHARMM36m: an improved force field for folded and intrinsically disordered proteins. Nature Methods 14(1), 71–73 (Jan 2017). https://doi.org/10.1038/nmeth.4067

13. Humphrey, W., Dalke, A., Schulten, K.: VMD: Visual molecular dynamics. Journal of Molecular Graphics 14(1), 33–38 (1996). https://doi.org/10.1016/0263-7855(96)00018-5

14. Jasprova, J., Dal Ben, M., Vianello, E., *et al.*: The biological effects of bilirubin photoisomers. PLOS ONE 11(2), 1–16 (02 2016). https://doi.org/10.1371/journal.pone.0148126

15. Jóźwiak, K., Ogrin, P., Urbic, T., Filarowski, A.: Molecular dynamics and density functional theory studies of conformational stability of bilirubin and biliverdin. Journal of Molecular Liquids 391, 123287 (2023). https://doi.org/10.1016/j.molliq.2023.123287

16. Lemli, B., Lomozová, Z., Huber, T., *et al.*: Effects of Heme Site (FA1) Ligands Bilirubin, Biliverdin, Hemin, and Methyl Orange on the Albumin Binding of Site I Marker Warfarin: Complex Allosteric Interactions. International Journal of Molecular Sciences 23(22), 14007 (Nov 2022). https://doi.org/10.3390/ijms232214007

17. Lin, Y.S., Li, G.D., Mao, S.P., Chai, J.D.: Long-range corrected hybrid density functionals with improved dispersion corrections. Journal of Chemical Theory and Computation 9(1), 263–272 (2013). https://doi.org/10.1021/ct300715s

18. Melo, M.C.R., Bernardi, R.C., Rudack, T., *et al.*: NAMD goes quantum: an integrative suite for hybrid simulations. Nature Methods 15(5), 351–354 (May 2018). https://doi.org/10.1038/nmeth.4638

19. Moosavi-Movahedi, Z., Bahrami, H., Zahedi, M., *et al.*: A theoretical elucidation of bilirubin interaction with HSA's lysines: First electrostatic binding site in IIA subdomain. Biophysical Chemistry 125(2), 375–387 (2007). https://doi.org/10.1016/j.bpc.2006.09.013

20. Morozenko, A., Stuchebrukhov, A.A.: Dowser++, a new method of hydrating protein structures. Proteins: Structure, Function, and Bioinformatics 84(10), 1347–1357 (2016). https://doi.org/10.1002/prot.25081

21. Petersen, C.E., Ha, C.E., Harohalli, K., *et al.*: A dynamic model for bilirubin binding to human serum albumin *. Journal of Biological Chemistry 275(28), 20985–20995 (Jul 2000). https://doi.org/10.1074/jbc.M001038200

22. Phillips, J.C., Hardy, D.J., Maia, J.D.C., *et al.*: Scalable molecular dynamics on CPU and GPU architectures with NAMD. The Journal of Chemical Physics 153(4), 044130 (07 2020). https://doi.org/10.1063/5.0014475

23. Radibratovic, M., Minic, S., Stanic-Vucinic, D., *et al.*: Stabilization of human serum albumin by the binding of phycocyanobilin, a bioactive chromophore of blue-green alga spirulina: Molecular dynamics and experimental study. PLOS ONE 11(12), 1–18 (12 2016). https://doi.org/10.1371/journal.pone.0167973

24. Seritan, S., Bannwarth, C., Fales, B.S., *et al.*: TeraChem: Accelerating electronic structure and ab initio molecular dynamics with graphical processing units. The Journal of Chemical Physics 152(22), 224110 (06 2020). https://doi.org/10.1063/5.0007615

25. Vanommeslaeghe, K., MacKerell, A.D.J.: Automation of the CHARMM General Force Field (CGenFF) I: Bond Perception and Atom Typing. Journal of Chemical Information and Modeling 52(12), 3144–3154 (2012). https://doi.org/10.1021/ci300363c

26. Wei, Y.l., Li, J.q., Dong, C., *et al.*: Investigation of the association behaviors between biliverdin and bovine serum albumin by fluorescence spectroscopy. Talanta 70(2), 377–382 (Sep 2006). https://doi.org/10.1016/j.talanta.2006.02.052

27. Wu, N., Zhang, R., Peng, X., *et al.*: Elucidation of protein–ligand interactions by multiple trajectory analysis methods. Phys. Chem. Chem. Phys. 26, 6903–6915 (2024). https://doi.org/10.1039/D3CP03492E

28. Zunszain, P.A., Ghuman, J., McDonagh, A.F., Curry, S.: Crystallographic Analysis of Human Serum Albumin Complexed with 4Z,15E-Bilirubin-IX. Journal of Molecular Biology 381(2), 394–406 (2008). https://doi.org/10.1016/j.jmb.2008.06.016